THE ASTROPHYSICAL JOURNAL, 324:75–92, 1988 January 1

COMPARATIVE PROPERTIES OF VIRGO CLUSTER DWARF IRREGULARS AND SPIRALS

G. LYLE HOFFMAN
Lafayette College
GEORGE HELOU
Infrared Processing and Analysis Center, California Institute of Technology
AND
E. E. SALPETER
Center for Radiophysics and Space Research, Cornell University
Received 1987 March 26; accepted 1987 June 20

ABSTRACT

We analyze the optical and neutral hydrogen data for all spiral and late-type dwarf irregular galaxies in the Virgo Cluster catalog. In particular, we examine the continuity of optical properties, hydrogen masses, and dynamical properties as functions of morphology and luminosity from the largest spirals through the faintest dwarfs (omitting blue compact dwarf galaxies); the effects of environment on H I content; mass segregation; and the Tully-Fisher relations. The spiral plus dwarf sample forms a continuous but nonhomologous sequence. Indicative dynamical mass-to-light ratios (obtained from central beam H I profile widths and *optical* radii) are relatively constant throughout; hydrogen mass-to-light ratios show only a slight increase with decreasing luminosity. The Tully-Fisher relations extend with continuous slope from spirals through dwarfs. The dwarfs show some evidence of ram-pressure stripping by the intracluster medium, but as a group do not seem to be stripped more heavily than spirals. There is no evidence of mass segregation even for the very low mass dwarfs versus giant spirals.

Some recent theories of the formation of dwarf galaxies are discussed in the light of this analysis.

Subject headings: galaxies: clustering — galaxies: formation — galaxies: internal motions — radio sources: 21 cm radiation

I. INTRODUCTION

Previous systematic H I surveys of dwarf irregular galaxies have either concentrated on low surface brightness objects (Thuan and Seitzer 1979; Fisher and Tully 1975; Huchtmeier, Seiradakis, and Materne 1981) or objects with blue high surface brightness patches (Thuan and Martin 1981). Recently a systematic optical study of all types of galaxies, including both dwarf ellipticals and dwarf irregulars, has become available for the Virgo Cluster and its immediate surroundings. This study appeared in a series of papers giving both a detailed classification scheme and atlas (Sandage and Binggeli 1984) and the full catalog (Binggeli, Sandage, and Tammann 1985, hereafter BST). In a previous paper (Hoffman *et al.* 1987, hereafter HHSGS) we gave the raw data from an extensive H I survey of all late-type spiral galaxies and dwarf irregular galaxies. The present paper contains a statistical analysis of much of those data. A preliminary discussion was given in Hoffman *et al.* (1985), and Bothun *et al.* (1985) gave a similarly preliminary account of a smaller subset of these galaxies.

The BST catalog and classification scheme cover a wide range of types and magnitudes from giant spirals to the faintest dwarf irregulars. The optical results are discussed in § II, and the H I results are discussed in § IV. In § III we discuss the necessary corrections to the raw data. We shall conclude that there is no discontinuity in the range of types but shall find it useful to define three broad groups: "SM" (which would include the Large Magellanic Cloud), "ImBr," and "ImFt" (the latter two of which include Magellanic irregulars of higher and lower surface brightness). A fourth group, pure bright, blue, compact dwarfs (hereafter BCD) will be discussed in detail in a later paper.

The survey region can be subdivided into an inner region, representing a relatively high density environment, and an outer region of lower density (although many of the galaxies in the latter are probably still members of the Virgo cluster). The IN/OUT comparison, presented in § V, is related to three kinds of possible environmental effects: (1) dependence of morphology on matter density at the time of formation of the cluster; (2) mass segregation during the epoch of "violent relaxation" and thereafter; and (3) ram-pressure stripping of interstellar gas by the intracluster gas. Our attempt at disentangling these three effects will be helped by some properties of the sequence of dwarfs: all dwarfs are probably of low enough mass that mass segregation should already be occurring between true spirals and Sm, whereas surface brightness (important for ram-pressure stripping) drops appreciably only between ImBr and ImFt. The ram-pressure stripping model is considered explicitly in § V, and mass segregation and other dynamical matters are discussed in § VI.

The Tully-Fisher (TF) correlation (Tully and Fisher 1977) between H I profile width and B_T magnitudes has found widespread application as a tertiary step on the distance ladder (Bottinelli *et al.* 1986; Aaronson and Mould 1983; Richter and Huchtmeier 1983; Giraud 1986*a*, *b*). In § VII we examine the extension of the TF correlation to very narrow profiles. This finds immediate application in assessing whether or not the blueshifted dwarf galaxies (along with the well-studied blueshifted bright spirals; Helou, Salpeter, and Krumm 1979, and references therein) lie in the foreground, and whether or not a number of high-velocity OUT spirals and dwarfs lie in the background.

We conclude with a discussion and summary in § VIII.

II. MORPHOLOGY AND OPTICAL PROPERTIES OF THE SAMPLE

Our observing sample is based on the BST catalog. A total area of ~ 140 deg^2 is included in the catalog; we divide this area into an "IN" region or cluster core, that portion within a circle of radius 5° centered on 12^h30^m, 13°0, and an "OUT" region incorporating the rest of the BST survey area. The catalog contains 152 "member" or "possible member" galaxies labeled "Sab" to "Sd" (which we call "spirals") and 293 galaxies labeled "Sdm" or later, including BCDs and the mixed type dE or Im. We call these 293 "dwarfs" (short for "dwarf irregular," since no dE dwarfs are included) regardless of their luminosities.

The classification scheme used in the BST catalog, described and illustrated in Sandage and Binggeli (1984), is based primarily on morphology, partly on surface brightness for BCDs and to determine the luminosity class, but not at all on absolute size or luminosity. BST give major optical diameters $D_{\rm est}$, hereafter denoted a, from which we construct a "face-on" optical surface brightness $\sigma_{\rm opt} = L/[(\pi/4)a^2]$. However, $(\pi/4)a^2$ represents an "outermost face-on area" rather than an isophotal area, and $\sigma_{\rm opt}$ is a "mean outermost surface brightness." Our $\sigma_{\rm opt}$ is thus quite different from (and smaller than) a central peak or even "effective" surface brightness; since the H I disk usually extends beyond the bright optical disk, $\sigma_{\rm opt}$ is a convenient measure for our discussion. In Figures 1 and 2 a number of mean properties are displayed, plotted against morphological type on the left, against apparent magnitude B_T on the right. For the fine binning of types in Figure 1, the first seven columns (through ImV) form a sequence from "early" to "late," but the remaining five columns are *not* meant as a continuation of this sequence. For the cruder binning in Figure 2, we have lumped Sb, Sbc together as Sb; Sc, Scd, Sd as Scd; Sdm, Sm as Sm; ImIII, III–IV, IV and all Im? with $\sigma_{\rm opt} > 2.5 \times 10^7\ L_\odot\ {\rm kpc}^{-2} = 23.5$ mag arcsec^{-2} as ImBr; and ImIV–V, V, and Im? with $\sigma_{\rm opt} < 2.5 \times 10^7\ L_\odot\ {\rm kpc}^{-2}$ as ImFt. We keep "pure" BCD galaxies as a separate type but assign S .../BCD to the corresponding S ... bin, and Im .../BCD to the corresponding Im ... bin. The type dE or Im is omitted from Figure 2.

Figures 1 and 2 (*right*) include a plot of a mean morphological type index $\langle t\rangle$ versus B_T (*row 6*). This is defined to be the index T as defined in RC2 for Sab–Sm ($t = T = 2$–9) and $t = 10$–14 for ImIII–ImV. Im? and Im: galaxies are divided according to their optical surface brightness, those brighter than the mean being assigned $t = 12$ and those fainter to $t = 14$. BCDs are assigned $t = 15$, while S .../BCD and Im .../BCD are assigned t according to the type of the underlying galaxy.

The mean values of $\sigma_{\rm opt}$, optical (angular) major diameter a, and apparent magnitude B_T are plotted against type in rows 4–6 in Figures 1 and 2 (*left side*). For the type BCD it is not always clear whether a measures the diameter of the whole galaxy or whether much of the galaxy has become so dim that a measures only the diameter of the bright patch. This type will be discussed in a later paper (Hoffman *et al.* 1988*a*). Disregarding BCD (as we shall do in most of the present paper), we see that $\langle a\rangle$ decreases monotonically and $\langle B_T\rangle$ increases monotonically with increasing "lateness" of type in Figure 2 (*left*). For our outer mean surface brightness $\sigma_{\rm opt}$, the small value for ImFt is partly due to the definition of types (as is the large value for BCD), but the first four rows contain a surprise: unlike averages for central, peak surface brightnesses (review by Gallagher and Hunter 1984; Kormendy 1985; Sandage 1983, 1986; Bothun *et al.* 1986), $\langle\sigma_{\rm opt}\rangle$, as defined here, does *not* decrease continuously with increasing "lateness," but is almost the same for Sm and ImBr as for the spirals.

This behavior of $\langle\sigma_{\rm opt}\rangle$ is not merely an artifact of the type definitions, as can be seen dramatically in Figure 1 (*right*): the thick ovals represent properties plotted against B_T, irrespective of morphological type, and the entries for $B_T \approx 15$–18 include some BCDs. The broken ovals (without error bars) to the right of the solid symbols give mean values with BCDs omitted entirely. Since the BCD type is selected for large $\sigma_{\rm opt}$, the broken ovals for $\langle\sigma_{\rm opt}\rangle$ from $B_T = 14$–18 should show a slight *downward* bias, if any. Even with this potential bias, $\langle\sigma_{\rm opt}\rangle$ for $14 < B_T < 16$ is *not* smaller than for the higher luminosity bins, whereas $\langle\sigma_{\rm opt}\rangle$ is decidedly smaller for $B_T > 18$ (where there is no bias). This behavior is consistent with $\langle\sigma_{\rm opt}\rangle$ remaining constant with type until ImBr and then dropping sharply for ImFt. Note also that the mean diameter $\langle a\rangle$ drops rapidly from spirals to Sm to ImBr, with a smaller drop to ImFt. The ratio $\langle\sigma_{\rm opt}\rangle/\langle a\rangle$, which would be a measure of the volume density of light *if* the thickness of each galaxy were proportional to a, thus *increases* from spirals to Sm to ImBr, but is quite small for ImFt. The central surface brightness, on the other hand, already drops from spirals to Sm, presumably because the irregular shape washes out strong central condensations (Binggeli, Sandage, and Tarenghi 1984; Sandage and Bingeli 1984; Bothun *et al.* 1986).

For various applications we need an estimate of the inclination angle i of each galactic disk, derived from an estimate of the axial ratio $R = a/b$. For many regular spirals the ratio R_{25} (de Vaucouleurs, de Vaucouleurs, and Corwin 1976, hereafter RC2) is known and the Holberg formula

$$\cos^2 i = \frac{[(R_{25})^{-2} - 0.04]}{(1 - 0.04)}, \qquad (1)$$

works well. For the dwarfs we have only the estimate $R_{\rm est}$ from BST for R and the irregular shape of dwarf irregulars means that even a face-on disk is not circular, so that R is likely to be appreciably larger than unity and equation (1) does not give $\sin^2 i = 0$ (see Grosbøl 1985; Feitzinger and Galinski 1986). Furthermore, edge-on dwarf galaxies presumably have an intrinsic b/a larger than 0.2 as assumed in equation (1). The distribution of inclinations we obtain for our sample based on equation (1), shown in Figure 3, is reasonably uniform for spirals, but shows the expected depletion of both face-on and edge-on dwarfs. For BCD, ImBr, and Sm, however, the mean $\langle\sin^2 i\rangle \approx 0.67$ as expected for a sample uniformly distributed in true inclination; for ImFt $\langle\sin^2 i\rangle$ is somewhat larger. Since we would expect edge-on ImFt either to be missing from BST (if there is any appreciable extinction in the disk) or to be classified as an earlier type (if there is little extinction), it seems reasonable to demand that the inclination formula we use for ImFt give the same $\langle\sin^2 i\rangle$ that we find for spirals. (This will be important for comparison of the dynamical properties.) We find that

$$\cos^2 i = \frac{R^{-2} - 0.2}{1 - 0.2} \qquad (2)$$

gives $\langle\sin^2 i\rangle \approx 0.67$ for ImFt, and so we adopt equation (2) for ImFt and equation (1) for the other morphological types.

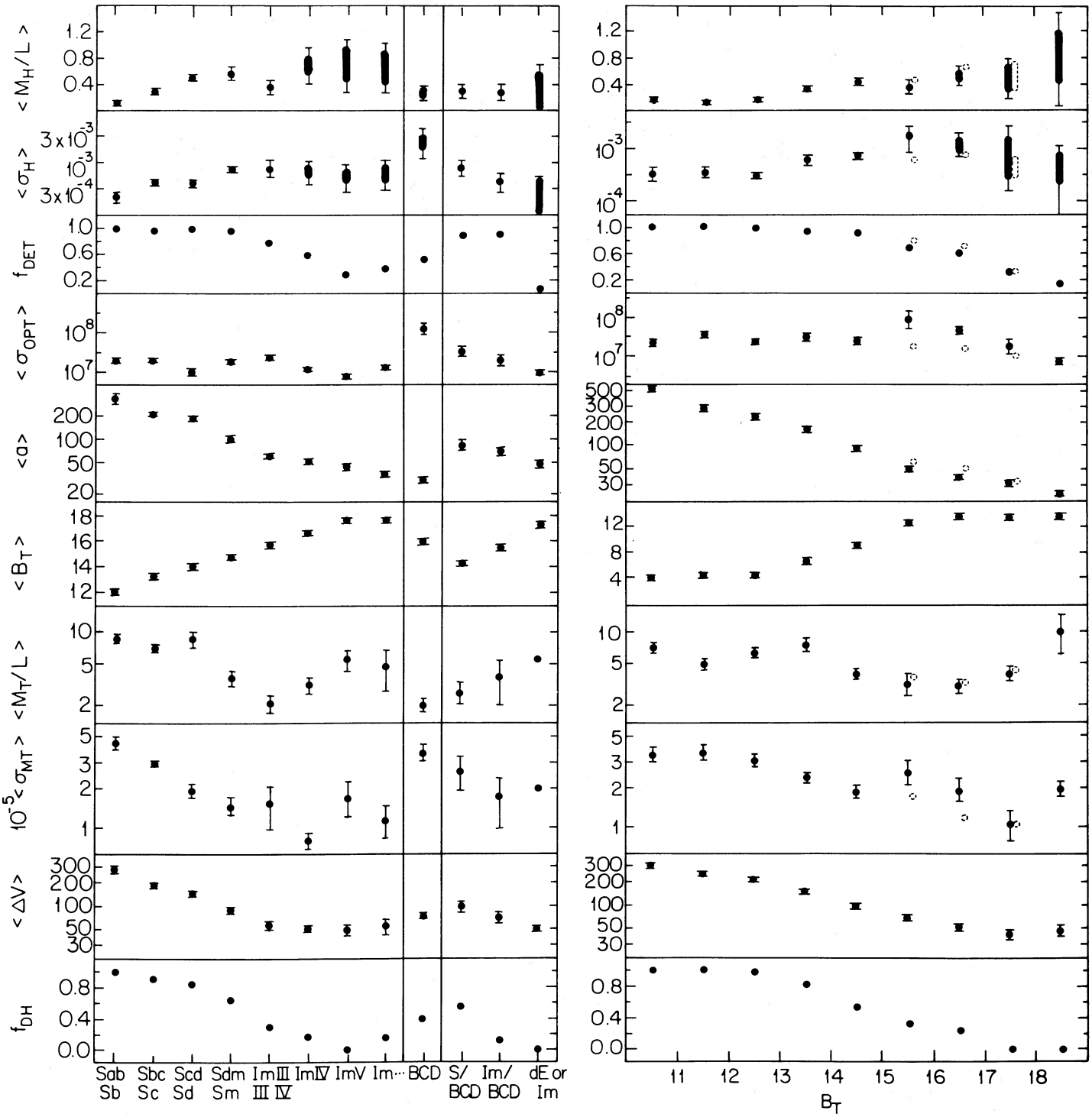

FIG. 1.—Mean optical, H I, and dynamical properties as a function of morphological type (*left*) and blue magnitude, corrected for inclination (*right*). See §§ II, IV for explanations of the various quantities. Oblong symbols for properties related to H I mass (*top two panels*) extend from the mean value with undetected galaxies counted at the full upper limit, to the mean assuming zero flux for nondetections. Broken symbols in the right-hand panels represent means with pure BCDs excluded. Units employed are, for ΔV, km s^{-1}; for σ_{MT}, $M_\odot$ kpc^{-2}; for M_T/L, solar units; for a, arc seconds; for σ_{opt}, $L_\odot$ kpc^{-2}; for σ_H, Jy km s^{-1} arcsec^{-2}; for M_H/L, solar units.

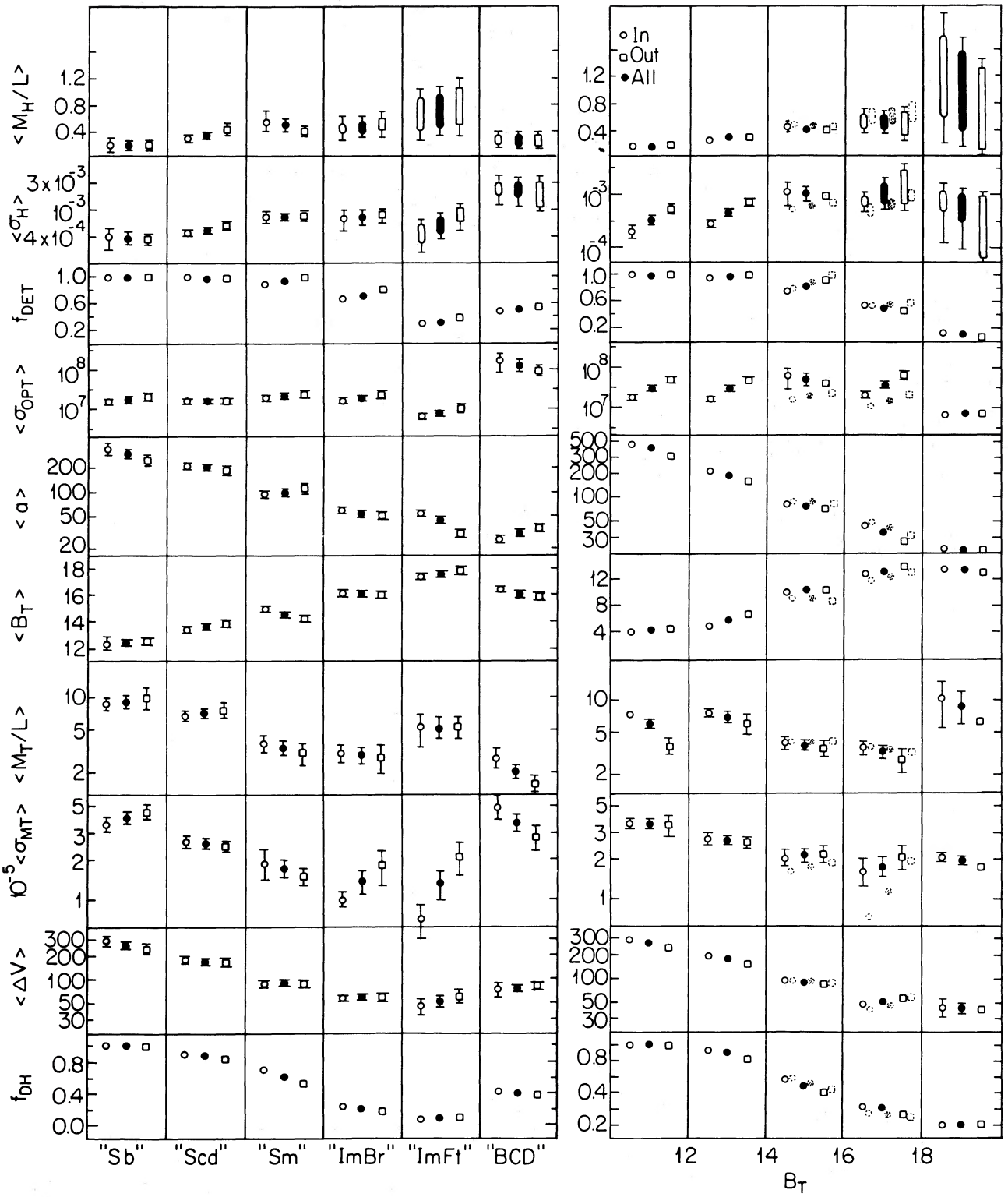

FIG. 2.—Same as Fig. 1, but with coarser morphology and magnitude bins and with galaxies inside (*open circles*) and outside (*open squares*) the 5° core shown separately.

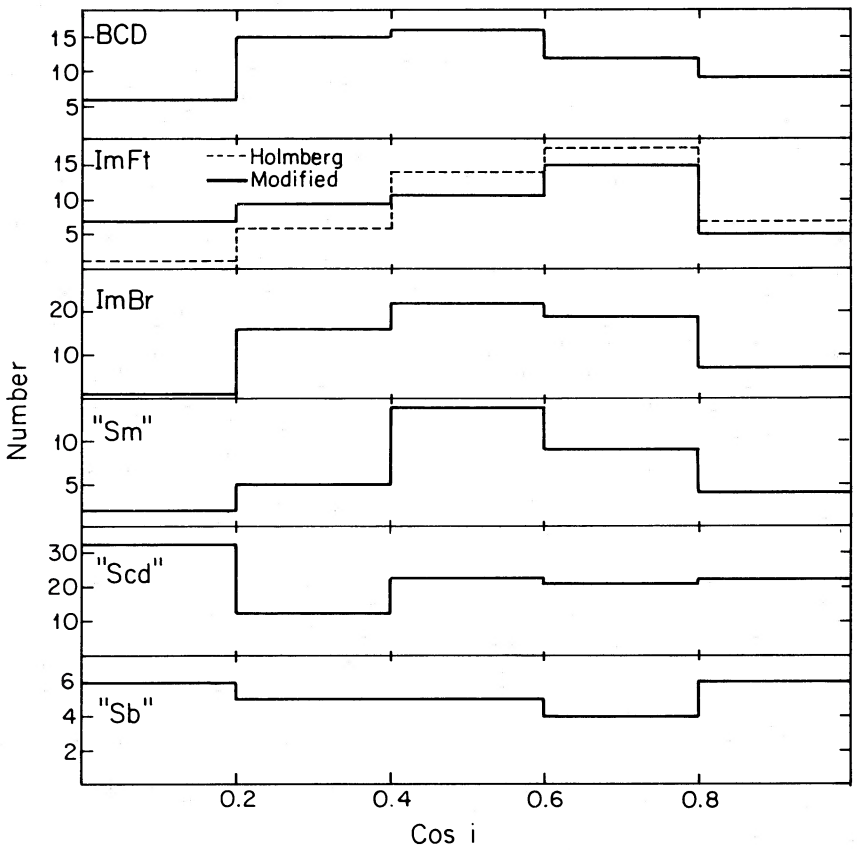

FIG. 3.—Distributions of the various morphological types in inclination angle. See § II for discussion of the assumptions made in determining i from the Holmberg formula and in modifying the formula for ImFt.

III. THE OBSERVATIONS AND CORRECTIONS TO THE DATA

We have now observed in the H I line all 293 late-type (Sdm on, plus dE or Im) galaxies cataloged by BST, using the Arecibo 305 m telescope[1] with the circularly polarized 1415 MHz line feed with ~ 15 km s^{-1} resolution after Hanning smoothing. Details of the observing and results for all dwarfs with $B_T \leq 17.0$, plus all known fainter ImV dwarfs, are given in HHSGS; the remaining faint objects (observed after HHSGS was written) will be reported on in a future paper. All the spiral galaxies classified in BST as Virgo Cluster member or possible member already have at least a central beam H I observation (Helou, Hoffman, and Salpeter 1984; hereafter HHS; Haynes and Giovanelli 1986; Hoffman *et al.* 1988*b*). The observational procedures were similar to those used for the dwarfs, and we use these spirals as a comparison sample.

For all the spirals with $B_T \leq 14.0$ we have H I mapping; for some of the fainter spirals and for only 42 of the dwarf galaxies, we have preliminary mapping data at 1.9 spacing (Hoffman *et al.* 1985). These data allow us (see HHS) to determine statistically a small factor for correction from central beam H I flux to a galaxy-wide total H I flux. For the 38 dwarfs that are *not* BCDs, we found a best-fit relation of the form

$$\log (f_{\rm tot}/f_c) = -0.035 + 0.217 \log a ,$$

where $f_c = \int Sdv$ is the observed flux (in mJy km s^{-1}) in the central beam alone, while $f_{\rm tot}$ is the integrated flux over the entire galaxy. The four mapped BCDs do not define a strong correlation of $f_{\rm tot}/f_c$ with major diameter, and so we adopt a simple mean correction factor for BCDs:

$$\langle \log (f_{\rm tot}/f_c) \rangle_{\rm BCD} = 0.0942 ,$$

irrespective of diameter. For the spirals we have a best-fit relation

$$\log (f_{\rm tot}/f_c) = 0.175 + 0.019 \log a .$$

For use in the Tully-Fisher relation and for obtaining dynamical masses, the observed H I profile widths at 50% of peak flux, ΔV_{50}, reported in HHSGS, must be corrected for resolution effects and for the galaxy inclination i. We use equation (2) for ImFt dwarfs and equation (1) for all other types. From computer simulations (including noise) we found an empirical relation between the measured ΔV_{50} and the intrinsic width at 50%, ΔV_I: $\Delta V_{50} - \Delta V_I = 2.0$ km s^{-1} for $\Delta V_{50} > 34$ km s^{-1}, and

$$\Delta V_{50} = 19.54 - 0.181 \Delta V_I + 0.0257 \Delta V_I^2 - 0.000179 \Delta V_I^3$$

for 20 km s^{-1} $\leq \Delta V_{50} < 34$ km s^{-1}. For $\Delta V_{50} < 20$ km s^{-1}, we adopt $\Delta V_I = 8$ km s^{-1}. Separating the true rotational velocity from the local velocity dispersion of the emitting gas is difficult for an individual galaxy (see review by Tully and Fouqué 1985), but we have some statistical information: for only two of our 293 dwarfs is the width ΔV_I (corrected for resolution but not inclination) less than 20 km s^{-1}, but $20 < \Delta V_I < 30$ km s^{-1} for 22 dwarfs. These 24 narrowest profiles (out of 293) are consis-

[1] The Arecibo Observatory is part of the National Astronomy and Ionosphere Center which is operated by Cornell University under contract with the National Science Foundation.

tent with the fraction expected to have $i \leq 10°$ in a sample uniformly distributed in orientation, so these widths are mainly dispersion and their mean is $\langle \Delta V_I \rangle = 25.0 \pm 1.1$ km s^{-1} (see also Huchtmeier, Seierdakis, and Materne 1980, 1981). Furthermore, estimates (Lewis 1975, 1984, 1987) of dispersion for giant spirals are remarkably similar to this value. We therefore adopt the following "hybrid" formula for a corrected velocity width ΔV_c,

$$\Delta V_c^2 = (\Delta V_{50}^2 - 25^2) \sin^{-2} i_c + 3(25^2) , \quad (3)$$

where the first term represents the inclination corrected rotational component and the second term represents the three-dimensional dispersion. To avoid overcorrecting face-on objects, we replace $\sin i_{\rm est}$ by 0.4 when $\sin i_{\rm est} < 0.4$.

Corrections for extinction to the galaxy magnitudes and sizes for the smallest dwarfs are uncertain at best. However, since we expect a bias against edge-on ImFt (but not against edge-on spirals), failure to correct the optical magnitudes for inclination could skew the comparisons of mass-to-light ratios, etc., for dwarfs versus spirals (de Vaucouleurs and Corwin 1986). We therefore adopt the RC2 corrections for extinction (using $R_{\rm est}$ from BST for the axial ratio) within each galaxy as a best available guess; these corrections depend directly on the observed axial ratios, not our inferred inclinations. At the high galactic latitude of the Virgo cluster, extinction within the Galaxy is unimportant (Burstein and Heiles 1984). We make no corrections to the optical diameters.

Only 19 out of the 168 dwarf galaxies we detected in H I have systemic velocities $V_\odot$ in excess of 3000 km s^{-1}. These are presumably behind the Virgo supercluster, and we do not include them in any tables, figures, analysis, or discussion in the present paper. In principle, some of the undetected galaxies could have $V_\odot > 3000$ km s^{-1}, but (*a*) the fraction at these velocities is small even for the detected ones, and (*b*) most of the undetected galaxies are ImIV and V, which typically have very faint absolute magnitudes, and few very distant ones are likely to be included in the BST catalog. For statistical purposes we therefore assume that all our undetected galaxies also have $V_\odot < 3000$ km s^{-1}. For all IN galaxies, i.e., those within 5° of the cluster center (R.A. = 12^h30^m, decl. = 13°0), and for those OUT galaxies (>5°, but in BST) with $V_\odot < 1900$ km s^{-1}, we assume a common distance $d_{\rm Virgo}$. No doubt a few of the OUT galaxies with $V_\odot < 1900$ km s^{-1} lie in the foreground or background of the cluster; we expect the OUT region to contain a somewhat larger range of distances than IN (see Binggeli, Tammann, and Sandage 1987, hereafter BTS). We would not expect that range to extend as far as a factor of 2, however, and the Virgo distance should be a convenient average. Many of the OUT galaxies with $V_\odot > 1900$ km s^{-1} (but < 3000 km s^{-1}) presumably lie behind the Virgo cluster core (but still inside the supercluster). The 42 spiral plus dwarf irregular galaxies outside 5° having $3000 > V_\odot > 1900$ km s^{-1} have a median velocity of $\sim$2250 km s^{-1}, which would place them at twice the Virgo distance according to most Virgocentric flow models. There are, however, eight such galaxies with $V_\odot < 300$ km s^{-1}; if the velocity distribution of galaxies on the outskirts of the cluster is symmetric we therefore expect eight of the 42 high-velocity galaxies to be at the cluster distance, in the tail of the velocity distribution. This assumption lowers the mean distance of the high-velocity galaxies to $\sim$1.8 times that of the Virgo Cluster core. In § V we estimate (using TF correlations) the mean distance of these galaxies to be $\sim 1.62 d_{\rm Virgo}$. For most comparison purposes, the value of the Virgo distance does not matter, but for concreteness we assume $d_{\rm Virgo} = 21.9$ Mpc (Sandage and Tammann 1976, 1982).

IV. HYDROGEN AND DYNAMICAL MASSES

Properties related to hydrogen content are displayed in the top three panels in Figures 1 and 2. These show the fraction, $f_{\rm det}$, of galaxies in each bin that were detected, a mixed H I surface density $\sigma_{\rm H} = 4M_{\rm H}/\pi a^2$ (where a is the *optical* diameter as above and the hydrogen mass is $M_{\rm H} = 2.36 \times 10^5 D^2 \int Sdv$, D being the distance of the galaxy), and the hydrogen mass-to-light ratio $M_{\rm H}/L$. Virtually all the spirals are detected, and $f_{\rm det}$ falls off more or less monotonically with increasing "lateness." The oblong symbols reach from the mean $\sigma_{\rm H}$ or $M_{\rm H}/L$, taking undetected galaxies at their full upper limits for $M_{\rm H}$, to the mean, taking $M_{\rm H}$ to be 0 for those galaxies. The solid ovals in Figures 1 and 2 (*left*) show the variations of $\langle M_{\rm H}/L \rangle$ and $\langle \sigma_{\rm H} \rangle$ with increasing "lateness": both climb slowly through the sequence of spirals to the transition type Sm and are almost the same for ImBr; for ImFt the ratio $\langle M_{\rm H}/L \rangle$ is even larger, but the mixed surface density is smaller—in keeping with the small value of optical surface density for this class. The trend for the true spirals in Figures 1 and 2 is qualitatively in accord with the findings of Haynes and Giovanelli (1984) for a sample of relatively isolated galaxies (our numerical values of $\sigma_{\rm H}$ are not comparable because of our use of optical diameters instead of the H I diameters used by those authors). The numbers of galaxies in each morphological bin are given in Table 1.

The same data are displayed as a function of apparent magnitude B_T in Figures 1 and 2 (*right*). The quantity $\langle M_{\rm H}/L \rangle$ increases slowly with increasing magnitude for the total sample; with the BCD galaxies removed (*thin solid ovals*) the rise is a little steeper at first and is almost absent for $B_T > 16$. With the BCDs removed, $\langle \sigma_{\rm H} \rangle$ increases until $B_T \approx 15$, is constant until $B_T \approx 17$, and decreases beyond—reflecting the fact that $B_T > 16$ for most ImFt galaxies.

There are two previous H I surveys of dwarf irregular galaxies comparable to our survey (excluding BCD), but mainly from *outside* of the cluster environment: Fisher and Tully (1975, hereafter FT), listing Green Bank observations of all the DDO dwarf galaxies, and Thuan and Seitzer (1979, hereafter TS), with Green Bank data for galaxies listed as dwarfs in UGC (Nilson 1973). We have 12 DDO objects in common between our list and FT, mainly spanning types Scd to ImIII–IV. The six objects detected in common give a mean ratio of FT flux to ours of 0.94 ± 0.11 (excluding cases of possible confusion with a neighbor); the FT mean (distance-

TABLE 1

MORPHOLOGICAL STATISTICS

Morphology Bin	Number Excluding Background	Number Detected in Virgo
Sab, Sb	23	23
Sbc, Sc	87	85
Scd, Sd	34	34
Sdm, Sm	27	26
ImIII, III–IV	23	18
ImIV, IV–V	35	21
ImV	35	21
Im, Im?, Im:	28	11
BCD	58	30
S .../BCD	8	7
Im .../BCD	10	9
dE or Im	31	1

independent) value of M_H/L is 0.74 ± 0.03, in accord with our values for Scd to ImIII–IV. For the TS survey, plus bright dwarfs from Thuan and Martin (1981), we have seven objects in common with a mean ratio of their flux to ours of 0.88 ± 0.08. After raising all TS values by 14%, to adjust to our calibration, their mean M_H/L is 0.68 ± 0.05. The results of both FT and TS are thus similar to ours for a comparable range of morphological types.

There are, in addition, two compilations of all-sky data for objects similar to our BCDs: Thuan and Martin (1981, hereafter TM), giving Arecibo and Green Bank data for blue compact dwarf galaxies identified by Markarian, Haro, and Zwicky; and Gordon and Gottesman (1981, hereafter GG) with data from the same telescopes for a similar list of blue compact dwarf galaxies. For comparison purposes we consider only TM and GG objects detected at $V_\odot \leq 3000$ km s^{-1}. At the resolution of the PSS plates, from which those surveys were drawn, we cannot be sure that the more distant objects are genuinely comparable to the BCD objects identified by BST. The two objects in common between our list and TM are both BCDs; we have no objects in common with GG. The mean M_H/L for all TM and GG objects with $V_\odot < 3000$ km s^{-1} is 0.36 ± 0.03, consistent with our BCD bin.

For each detected galaxy we obtain two pieces of information relevant to the galaxy's internal dynamics: an indication of whether the profile is double horned, typical of large edge-on spirals, or Gaussian, typical of an unwarped spiral seen face-on; and the profile width ΔV_{50}. The fraction f_{DH} of detected profiles exhibiting double horns is shown in the bottom panels of Figures 1 and 2 for morphological and magnitude bins. The statistics that make up these two figures are limited to galaxies detected at redshifts appropriate to Virgo. In general, f_{DH} decreases toward the later and fainter galaxies, as expected and as found by FT and TS for samples of nearby dwarfs. This is due to the rotational velocity decreasing strongly along the sequence while the random dispersion remains essentially constant.

The profile width, after a correction for inclination as in § III, allows us to determine an "indicative" dynamical mass $M_T = \Delta V_c^2 a/8\pi G$. This quantity is displayed in Figures 1 and 2 in two guises: as a mixed surface density of dynamical mass $\sigma_{MT} = 4M_T/\pi a^2$, and as a mass-to-light ratio M_T/L. Both $\langle M_T/L\rangle$ and $\langle\sigma_{MT}\rangle$ decrease continuously and slowly from the early spirals to the ImBr types; the latest and faintest ImFt types have a strong increase in $\langle M_T/L\rangle$ so that $\langle\sigma_{MT}\rangle$ remains almost constant. It should be remembered that M_T is only an "indicative mass," i.e., the mass out to the optical radius, whereas the dominant dark matter may have an (unknown) larger radius. Preliminary H I mapping data (to be reported on later) indicate little systematic variation of the ratio of H I to optical radii along the morphological series.

A major feature of our results on internal dynamics is the absence of any discontinuity (or even strong change of slope) between true spirals and dwarf irregulars in $\langle M_T/L\rangle$. The one possible exception is the marked increase of $\langle M_T/L\rangle$ toward the ImV type, but it should be remembered that we have data only on the H I–detected galaxies and that the detected fraction is small for ImV (see also § V). Vigroux, Stasinka, and Comte (1987) argue from their study of heavy-element abundances in an all-sky sample of nearby dwarfs, that virtually all the dynamical mass M_T must have participated in the astration, so that either dwarfs do not have nonbaryonic dark matter, or M_T samples only the central regions of the galaxy. As a working hypothesis for dwarf irregulars as a whole, we can assume that the ratio of dark mass to stellar mass is not radically different from spirals, and, most certainly, dynamical masses are smaller for dwarfs than for spirals.

V. EFFECTS OF ENVIRONMENT

A number of studies (Guiderdoni 1987; Guiderdoni and Rocca-Volmerange 1985; Giovanardi *et al.* 1983; Chamaraux, Balkowski, and Gérard 1980; Davies and Lewis 1973; Haynes and Giovanelli 1986; see especially review by Haynes, Giovanelli, and Chincarini 1984) have shown that spiral galaxies in the Virgo Cluster core are deficient in H I compared to similar galaxies outside the core. H I mapping studies at Arecibo (Helou *et al.* 1981; Hewitt, Haynes, and Giovanelli 1983) and synthesis telescopes (van Gorkom and Kotanyi 1985; Warmels and van Worden 1984) found the deficiency to be due mainly to a decrease in H I radii (rather than in the peak H I column density). Studies of CO emission in the Virgo Cluster (Stark *et al.* 1986) show that H I deficient galaxies are *not* deficient in the denser molecular clouds. These two results suggest ram-pressure stripping of the gaseous disk of a spiral by the intracluster gas (visible in X-rays; see reviews by Giovanelli and Haynes 1985 and Sarazin 1986) as the main effect of the environment. The resistance of a disk galaxy to such stripping depends on a dimensionless parameter of the form

$$\xi = \frac{(\sigma_{HI}/a)\Delta V_e^{2+\beta}}{\rho_\infty V_\infty^{2+\beta}} \propto \frac{\sigma_{HI}\sigma_{MT}\Delta V_e^{\beta}}{V_\infty^{2+\beta}}, \quad (4)$$

where ΔV_e should be the escape velocity from the galaxy but can be replaced by a multiple of the H I velocity width ΔV_c (see eq. [3]). In equation (4) ρ_∞ is the density of the intracluster gas, V_∞ its velocity relative to the galaxy, before its approach to the galaxy. In the simplest models (Gisler 1976; Lea and DeYoung 1976) $\beta = 0$, but under other circumstances more appropriate to elliptical galaxies $\beta \approx 0.4$ (Gaetz, Salpeter and Shaviv 1987). For the episodic stripping expected for disk galaxies in the Virgo Cluster, β is not known, but is also likely to be small and positive.

As a simple test of the environmental effects, we compare equivalent galaxies inside and outside of the circle of 5° radius (IN vs. OUT). We find it preferable to adopt a "broad-brush" approach, rather than the fine-grained subdivision into regions of high and low density used by Dressler (1986) and BTS, to bolster the statistical significance of our results. Note also that the X-ray emission from Virgo, which presumably traces the dominant gravitational potential well and contributes in largest measure to the environmental effects, is centered on M87, near the center of our IN region. The numbers of galaxies IN and OUT in each morphological bin are detailed in Table 2. Although an appreciable fraction of the OUT galaxies in our BST sample are likely to be cluster members, most are likely not to have orbited through the dense inner Virgo Cluster core (within 2° of the center, say). This comparison for the mean H I (and dynamical) properties is given in Figure 2 for both the spirals and the dwarf irregulars (open ovals on the left for IN and open rectangles on the right for OUT). It should be noted that the product $\langle\sigma_H\rangle\langle\sigma_{MT}\rangle$ in equation (4) varies little from the bright, true spirals to ImBr; for ImFt all means are less reliable because the detected fraction f_{det} is small, but this product, and especially the combination $(\sigma_H\sigma_{MT}\Delta V_c^{\beta})$, is likely to be smaller than for the brighter morphological types.

Given the uncertainty in the envrionmental effects on the

blue light of the individual morphological types, it is best to focus on the hydrogen surface density as an indicator of H I deficiency (Haynes and Giovanelli 1984; Dressler 1986). In Figure 4 we show H I flux versus optical diameter (on log scales) for all morphological types (Sb through ImFt, excluding BCD), all $V_{\odot} \leq 3000$ km s^{-1}, for OUT and IN galaxies separately. Undetected galaxies are plotted at one-half the upper limit. The OUT galaxies (Fig. 4*b*) are well fitted by a straight line of slope 1.81; fits to the individual morphological types (shown with separate symbols in Fig. 4) confirm that this slope is reasonable for each type. The slope 1.81 is, however, *smaller* than any of the individual slopes, reflecting the slight morphological dependence of σ_H evident in Figures 1 and 2. The corresponding plot (Fig. 4*a*) for IN galaxies is well fitted by a line of the same slope, but the scatter is considerably larger, mostly due to a number of strongly deficient galaxies, both spirals and dwarfs (see also Haynes and Giovanelli 1986). The zero point is smaller than that for OUT galaxies by 0.25 ± 0.05. Corresponding plots of log M_T versus log a show no significant zero point difference.

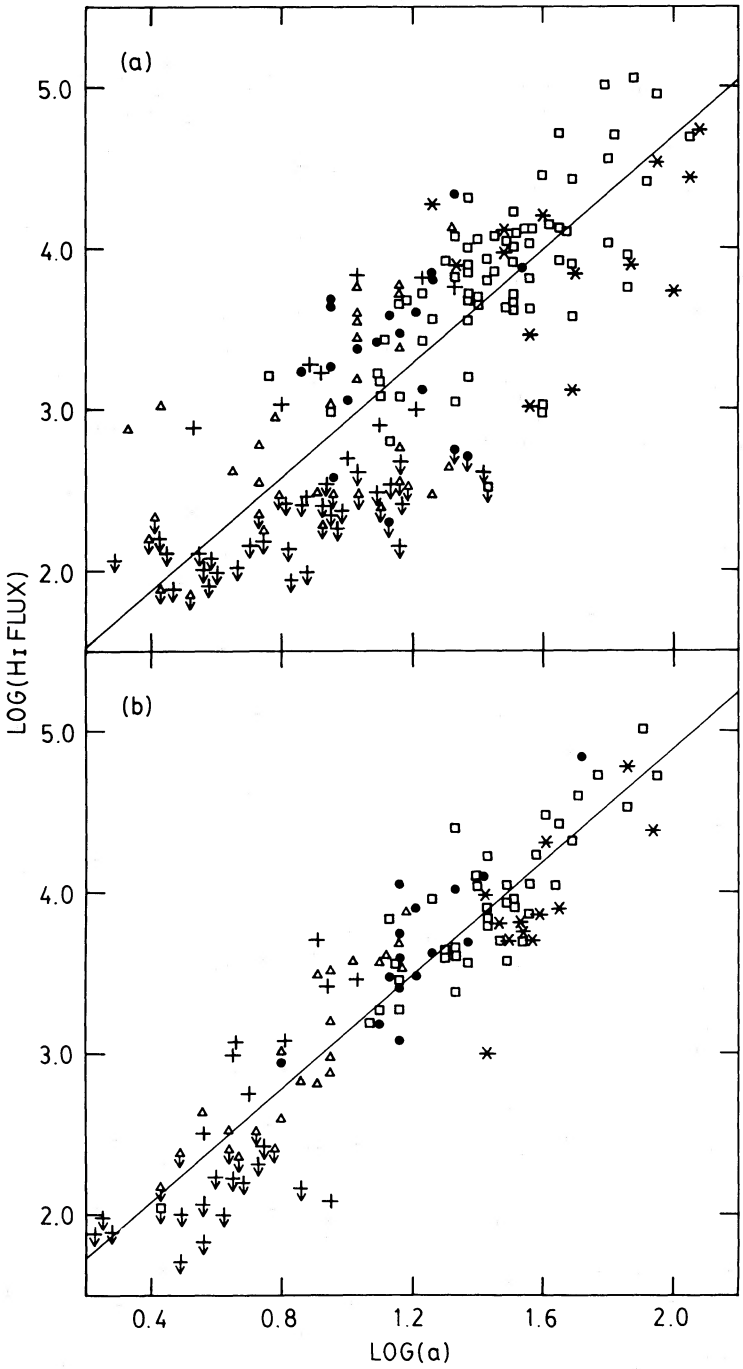

FIG. 4.—Scatter diagrams of H I flux vs. optical diameter a for (*a*) IN and (*b*) OUT galaxies separately. The line drawn for the OUT panel (*b*) is the best fit to those data; the line for the IN panel (*a*) is constrained to have the same slope as OUT, but a separately fitted zero point.

TABLE 2

IN/OUT STATISTICS

Type	Location	Number Excluding Background	Number Detected in Virgo
Sb	IN	21	21
	OUT	13	13
Scd	IN	69	68
	OUT	42	41
Sm	IN	19	17
	OUT	15	15
ImBr	IN	41	27
	OUT	26	21
ImFt	IN	41	12
	OUT	23	9
BCD	IN	26	12
	OUT	32	18

In Table 3 we give the difference in zero points (OUT minus IN) for the correlation of H I flux versus a, similarly computed for each broad morphology bin using the same fixed slope 1.81 for all. In this view, ImBr and ImFt both show the expected increase in deficiency over the spirals, not strongly, however, and with small formal significance.

The ram-pressure stripping model further suggests that galaxies with high velocity with respect to the intracluster gas should be more severely stripped than lower velocity objects (if they have passed through similar regions) (see Dressler 1986 and Giraud 1986*a*). We test this hypothesis by dividing the galaxies into velocity bins: "LOW," for $V_\odot < 300$ km s^{-1}; "HIGH," for 1900 km s^{-1} $< V_\odot <$ 3000 km s^{-1}; and "CENter," for $300 < V_\odot < 1900$ km s^{-1}. The significance of the effect is maximized if we shrink (for this purpose only) the IN region to 4° and combine LOW and HIGH into a single "EXTreme" bin. We have, for IN galaxies, 45 EXT and 53 CEN with Δ(zero point) $= 0.16 \pm 0.09$ (CEN − EXT); for OUT galaxies, 48 EXT and 78 CEN, we have Δ(zero point) $= -0.15 \pm 0.07$.

The cluster environment has affected the color distribution of the dwarf galaxies as well (Gallagher and Hunter 1986), and it seems reasonable to suppose that H I deficient dwarfs have been reddened also by the cessation of star formation. To test this hypothesis, we correlate H I deficiency against optical colors $U-B$ and $B-V$ for the 41 objects in common between our list and that of Gallagher and Hunter (1986). BCDs, spirals, and background objects are excluded from this analysis. Defining DEF to be $\log (M_H/M_{H,\text{expected}})$, where $M_{H,\text{expected}}$ is determined by morphological type and optical diameter of OUT galaxies as in Giovanelli and Haynes (1985), we find DEF $= 0.48 - 1.39(B-V)$ (correlation coefficient $r = -0.46$) and DEF $= -0.37 - 1.66(U-B)$(for $r = -0.59$).

TABLE 3

H I DEFICIENCY

Morphological Bin	Number IN	Number OUT	Intercept Difference
Sb	14	12	0.15 ± 0.18
Scd	69	42	0.14 ± 0.06
Sm	19	15	0.19 ± 0.14
ImBr	34	23	0.25 ± 0.11
ImFt	42	23	0.29 ± 0.12

These results for our late-type dwarfs, compared with true spirals, can be summarized as follows: (1) as for spiral galaxies, there are *some* manifestations of environmental effects; for the dwarfs this manifestation is primarily a smaller detection fraction f_{det} IN than OUT; (2) at least for the brighter dwarf types, "Sm" and ImBr in Figure 2, the mean deficiency is at most slightly stronger than for spirals; (3) for the dwarf types with low surface brightness, ImFt, we cannot say at the moment whether the deficiency is stronger than for spirals or not, because of two opposite facts: (*a*) for those galaxies definitely classified as ImFt and detected in H I, the deficiency is *not* stronger; (*b*) BST list 29 galaxies IN but only two galaxies OUT as morphological type dE or Im, and all but one of these 31 galaxies are *undetected* in H I. (By contrast, galaxies listed as dE [or dS0] by BST number 874 IN and 268 OUT, intermediate between late-type dwarfs and the dE or Im type.) The dE or Im type of dwarf has very low optical surface brightness, like dE and ImFt, but unlike ImBr. It is then quite plausible that this morphological type is the result of extensive ram-pressure stripping some time ago, turning off star formation in ImIV or ImV galaxies (Vigroux *et al.* 1986; Binggeli 1985). The spectacular IN/OUT disparity in numbers for dE or Im would then indicate a strong H I deficiency.

It is tempting to carry this argument further, to claim that the eventual result of stripping of a dwarf irregular is an object indistinguishable from a dE (Kormendy 1985; Lin and Faber 1983). There are three arguments against this, however: (1) ram-pressure stripping cannot account for nucleated dEs (Binggeli 1985), nor the general tendency for greater *central* surface brightness in dE than in dwarf irregular galaxies (Bothun *et al.* 1986); (2) the velocity distribution of stripped galaxies should be broader than that of galaxies which still retain their gas, whereas the histograms of Figure 6 show dEs to have a more sharply peaked distribution than the irregulars; (3) If any substantial fraction of the dEs were so produced, the ratio of numbers of dI to spirals IN versus OUT should show a much greater disparity (see also Bothun *et al.* 1986 and Gallagher and Hunter 1986). The possibility remains, however, that stripping has produced a *small* fraction of the non-nucleated dEs (and in fact the extreme velocities in the cluster do belong to dEs).

Besides the several points just made, there are other finer points in Figure 2, especially those involving σ_H and σ_{MT}. However, these should *not* be taken seriously at the moment—partly because the formal level of significance is not strong and partly for another puzzling disparity: some of the optical properties in Figure 2, especially $\langle \sigma_{\text{opt}} \rangle$ and $\langle B_T \rangle$ for a given morphological type, also show IN/OUT differences. Some of these show opposite trends for adjacent types and any further discussion would be premature (see also Bosma 1985).

VI. MASS SEGREGATION AND CLUSTER DYNAMICS

N-body results (Farouki and Salpeter 1982; Farouki, Hoffman, and Salpeter 1983) show that mass segregation occurs during violent relaxation, even before two-body relaxation effects have become important, if all the dynamical mass of the cluster is concentrated around individual galaxies. While there is evidence that some of the spirals and dwarfs are recent arrivals in the cluster (Tully and Shaya 1984), the H I deficiencies discussed above make it clear that a substantial number of these galaxies must have passed through the cluster core at least once, participating in the violent relaxation, and should therefore exhibit a small but marginally detectable

amount of mass segregation if a sufficient dynamic range of masses is observed. These simulations show that "medium-light" and "light" particles behave similarly, in contrast only with the "heavy" particles. Mapping results (Helou, Hoffman, and Salpeter 1987; Skillman and Bothun 1986) and Figures 1 and 2 argue that the dynamical mass-to-light ratios for these dwarf galaxies are not significantly larger than for spirals. The dwarf-plus-spiral sample should thus have sufficient dynamic range to test whether or not mass segregation is present, even if we omit all ImFt and dE or Im galaxies to minimize indirect effects of ram-pressure stripping. There are two effects to be sought: the lighter particles should tend to lie at greater radii from the center of the cluster than the more massive spirals, and at any given radius the light particles should have a larger velocity dispersion σ_V than the spirals.

Figure 5 consists of maps of the cluster for E + dE + S0,

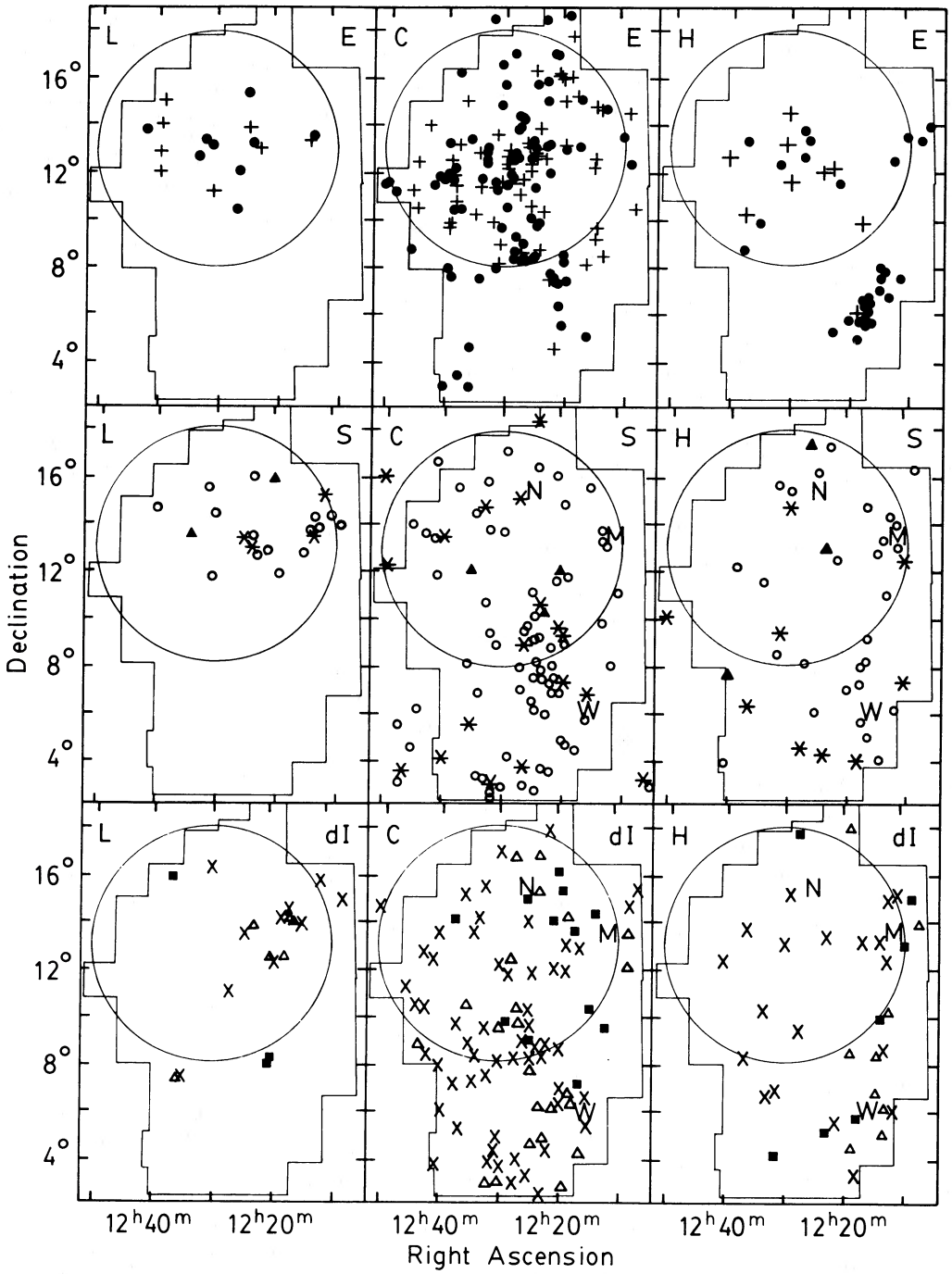

FIG. 5.—Maps of the Virgo Cluster for various morphological types and velocity ranges. Panels labeled "L" show galaxies with $V_\odot \leq 300$ km s^{-1}, those labeled "C" have $300 < V_\odot \leq 1900$ km s^{-1}, and those labeled "H" have $1900 < V_\odot \leq 3000$ km s^{-1}. Panels marked "E" in the upper right corner include dE (*crosses*) and E, S0, and Sa galaxies (*solid circles*); "S" panels include Sab and Sb (*asterisks*), Sbc and Sc (*open circles*), and Scd and Sd (*solid triangles*); and "dI" panels include Sdm, Sm, and ImBr (*exes*), ImFt (*solid squares*), and BCD (*open triangles*). The centers of the M, N, and W clouds are marked for the "C" and "H" velocity maps. The irregular boundary marks the limits of the BST survey area, and the circle delineates the 5° core.

spiral (Sab–Sd) and late-type dwarfs, respectively. Each map comes in three parts, for the LOW, CENTER and HIGH velocities of the previous section. A great deal of subclustering is evident: this is not new (de Vaucouleurs 1961; de Vaucouleurs and de Vaucouleurs 1973; Huchra, Davis, and Latham 1984; Huchra 1985; Tanaka 1985*a*, *b*). Morphological segregation is also quite apparent; the cluster center is much better defined by the dE galaxies than by the spirals or dwarf irregulars, as has been pointed out by others (Sandage, Binggeli, and Tammann 1985). Two of the clumps evident in the HIGH velocity maps are known to lie in the background; these are the W cloud (de Vaucouleurs 1961; de Vaucouleurs and de Vaucouleurs 1973; de Vaucouleurs and Corwin 1986), evident as a dense knot at 12^h18^m, 6° in the E + dE + S0 map, and the M cloud (Ftaclas, Fanelli, and Struble 1984), a more diffuse grouping that may include E + dE + S0 and dI as well as spiral galaxies, near 12^h10^m, 13°; the N cloud (Ftaclas *et al.*) may also lie somewhat behind the cluster core.

A quick comparison of the spiral and dI maps shows no pronounced differences in the distributions on the sky. Certainly *some* of the dI clumps correlate well with spirals, e.g., those near 12^h25^m, 9° and in the southern extension at 12^h30^m, 4°. There is an interesting positional coincidence between a cloud of dIs at 12^h20^m, 6° with the much tighter W cloud evident in the HIGH velocity E map; the dIs, however, are at somewhat lower velocities. A more detailed comparison of the dI velocities in this cloud shows that it comprises *two* subclouds, one with velocities near the boundary between CEN and HIGH (1900 km s^{-1}) and another more typical of the cluster mean, ~900 km s^{-1}. More quantitatively, counting all velocities $V_\odot \leq 3000$ km s^{-1}, we have 77 dI IN versus 74 OUT (ratio 1.04), but 83 spirals IN versus 60 OUT (1.38). Restricting velocities to the 300–1900 km s^{-1} range to avoid background contamination of the OUT sample, we have for dwarfs 50 IN versus 44 OUT (1.14), while for spirals we have 41 IN versus 40 OUT (1.02). Bearing the above discussion of H I deficiencies in mind, we cannot discern any evidence in these numbers for mass segregation. The velocity dispersion of dwarfs IN is 766 km s^{-1} versus 845 km s^{-1} for the spirals, again providing no evidence for mass segregation. (Restricting the dwarf sample to Sm and ImBr only gives a velocity dispersion of 759 km s^{-1}; the 12 detected ImFt IN have a dispersion of 828 km s^{-1}.)

TABLE 4

VELOCITY MEANS AND DISPERSIONS FOR THE 5° CORE

Type	Mean $V_\odot$ (km s^{-1})	Dispersion (km s^{-1})
All	1135 ± 41	733
E + dE + S0 ..	1161 ± 51	647
Sab–Sd	1116 ± 93	845
Sdm–ImV	1101 ± 88	766

Velocity histograms are shown in Figure 6, broken down by morphological type and position IN or OUT. Velocities for a number of dE galaxies and for a few undetected dIs were provided by Huchra (1984).

Mean velocities and dispersions for galaxies in the inner 5° are given in Table 4, broken down by morphological type. The W cloud is entirely excluded by the 5° circle, as is much of the M cloud. We find no significant difference in mean velocity for the three large morphological subdivisions, although the dispersions and shapes of the histograms are quite different. Since there is clearly antisegregation for the presumably very low mass dE galaxies with respect to massive spirals, and, if anything, antisegregation for the dI galaxies as well, we conclude that the galaxy velocities have retained some memory of the different formation and evolutionary histories of the different morphological types (see also Tanaka 1985*b*; Tully and Shaya 1984).

VII. TULLY-FISHER RELATIONS AND THE STRUCTURE OF THE VIRGO SUPERCLUSTER

The difficulty of assigning inclinations to the dwarf galaxies (§ III) and the lack of photometric magnitudes and diameters for all but a handful of galaxies would make any attempt at using this dwarf sample to determine a precise slope or zero point of the TF relation questionable at best. However, by accepting a larger scatter than would usually be permitted in TF studies (Tully and Fisher 1977; Bottinelli *et al.* 1986; Aaronson and Mould 1983; Richter and Huchtmeier 1984; Tully and Fouqué 1985; Giraud 1986*a*, *b*), we can use TF to assess whether or not the dwarfs are a continuation of the sequence defined by the spirals and whether or not the HIGH

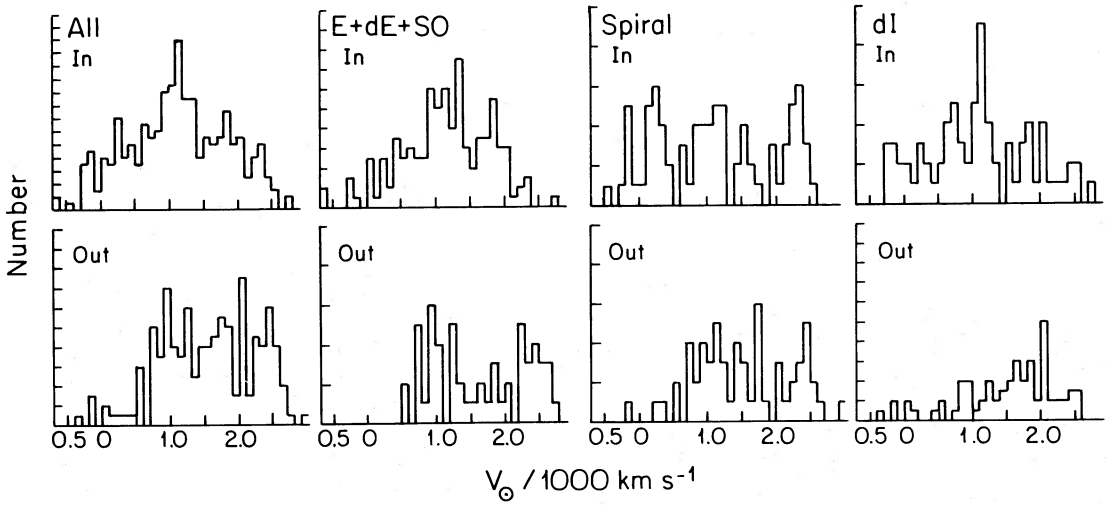

FIG. 6.—Velocity histograms IN and OUT of the 5° core, for all morphological types combined and for early, spiral, and irregular types separately

and LOW velocity groups (§ V) are in fact at the same distance from the Local Group as the CENter group.

Inclination corrections are discussed above in § III. We use the modified Holmberg formulae (1) and (2) and apply a lower limit of 0.4 on sin i to avoid overcorrecting face-on objects. Corrections to B_T and the velocity widths are discussed in § III; we make no corrections to the major diameter a.

Figure 7*a* shows the TF diagram, B_T versus log (ΔV_c) for the dwarf + spiral sample (excluding BCD and Sab), IN and OUT, including all velocities $V_\odot \leq 3000$ km s^{-1}. OUT HIGH have had B_T and a adjusted for a distance larger than that to the Virgo core by a factor of 1.62, as above. Different symbols are used for each of the broad morphological classes. There are hints in these figures that minor morphological effects are present and contribute to the scatter; note in particular that ImFt galaxies tend to fall slightly above the best-fit line in Figure 7*a*, while Sm galaxies fall mostly below the line at the low profile width end. The scatter for all types is large, however, and there is no apparent distinction that can be drawn between the spiral and dwarf samples. The well-studied morphological dependence of the TF relation (Roberts 1978; Richter and Huchtmeier 1984, Aaronson and Mould 1983; Giraud 1986*b*; Bottinelli *et al.* 1986) is primarily due to the earliest types, Sa and Sab, which we have excluded. Any residual morphological dependence is swamped by the scatter. The corresponding TF plot of log (ΔV_c) versus log a is given in Figure 7*b*. Here again, despite the large scatter, there is no apparent distinction between dwarfs and spirals. Linear regression on B_T versus log (ΔV_c) gives $B_T = 24.91 - 5.064 \log (\Delta V_c)$, while linear regression on log a versus log (ΔV_c) gives $\log a = -1.880 + 0.677 \log (\Delta V_c)$.

A comparison of the scatter in dynamical and luminous parameters is relevant to various models of the formation and evolution of these dwarf galaxies. In particular, the stochastic self-propagating star formation model (Gerola, Seiden, and Schulman 1980; Comins 1984) would hold that dynamical mass should be tightly correlated with optical diameter, while the blue luminosity should vary widely depending on whether or not the galaxy has experienced a recent star formation burst. A scatter plot of M_T versus a (IN and OUT together) is given in Figure 8*b*; the variance of log M_T about the best-fit line is 0.36. Figure 8*a* gives the corresponding scatter plot of blue luminosity (log $L \propto -0.4B_T$) versus a; its variance is 0.29. However, the estimated *measurement* errors in log L (based mostly on the *estimated* B_T in BST) amount to only about ± 0.2, leaving an intrinsic scatter in log L of about ± 0.2. The errors in measuring ΔV_{50}, in determining sin i, and in interpreting ΔV_{50} as the dynamically relevant profile width (no matter what the profile shape) can easily account for the *entire* scatter in log M_T, so that these data do not contradict the self-propagating star formation scenario (see, however, Matteucci and Chiosi 1983).

To test for a substantial population of foreground or background objects, we fit a line of predetermined slope (-5.064 for B_T vs. log ΔV_c, 0.677 for log ΔV_c vs. log a) to the data for the CENter, HIGH, and LOW velocity groups independently, each for both IN and OUT. For this purpose only, we do *not* adjust B_T and a for the OUT group. The results are given in Table 5. For IN galaxies, there are no statistically significant differences in zero points for either B_T or log a (note that the W cloud, which contains few spiral or dI galaxies in any case, falls outside 5°). The four OUT LOW galaxies are too few to determine any statistically significant difference in zero point from the OUT CENTER group; the OUT HIGH group is ~ 0.8 mag fainter in the mean (significant at the 4 σ level) and 37% smaller in diameter (4.5 σ significance), both consistent with their lying $\sim 62\%$ further away in the mean. There are no statistically significant differences in B_T or log a for the CENTER group IN versus OUT. Note also that the scatter for OUT CEN is not significantly greater than for IN CEN, indicating that OUT CEN is not badly contaminated by galaxies at distances substantially greater than $d_{\rm Virgo}$.

TABLE 5

TULLY-FISHER RESULTS

Location	Velocity	Number	B_T Zero Point	log a Zero Point
IN	LOW	27	24.76 ± 0.16	-1.84 ± 0.05
IN	CEN	74	24.92 ± 0.11	-1.85 ± 0.04
IN	HIGH	30	24.95 ± 0.17	-1.89 ± 0.08
OUT	LOW	4	25.48 ± 0.70	-1.86 ± 0.10
OUT	CEN	63	24.95 ± 0.11	-1.91 ± 0.04
OUT	HIGH	28	25.81 ± 0.24	-2.13 ± 0.06

The TF diagrams are shown for the individual groups in Figures 9 (B_T) and 10 (log a). OUT LOW are not shown separately since there are so few galaxies represented. OUT HIGH have B_T and a adjustments for distance applied. These answer some questions that might be raised in the preceding paragraph: (1) the scatter is about the same for every group, and so is due to intrinsic scatter in the properties of the galaxies or to measurement uncertainty, not to the inclusion of galaxies at various distances; (2) the common slopes used above fit each group equally well; there are no evident breaks between spirals and dwarfs in any group. Differences in slope and zero point for different morphological types within the range Sb to ImFt are small compared to the scatter.

VIII. DISCUSSION AND SUMMARY

One of the prevading questions about dwarf galaxies is: What is their connection to the larger, also gas-rich spirals? It is frequently supposed (e.g., Gallagher and Hunter 1984) that the absence of a spiral pattern in dwarf irregulars is due to a lower specific angular momentum for the dwarfs than for spirals. In applications of the TF relations, especially to nearby groups (e.g. Richter and Huchtmeier 1984) it becomes quite important to know whether the same relations extend through dwarfs, so that the substantial numbers of dwarfs can be used to bolster confidence in the distances obtained, or whether there is a break in the relation at some velocity width ΔV below which dwarfs predominate. A break in the relation might also be expected if ordinary neutrinos with a finite mass should constitute the dark matter in giant spirals, since dwarfs have too small a mass for this to be possible.

Two trends characterize the sequence from late spiral galaxies (Sb, say) through the faintest dwarf irregular type ImV (but omitting the pure BCD type): (1) There are *no* sharp discontinuities in any of the mean properties as a function of type (or magnitude), displayed in Figures 1 and 2. Similarly, there are no "kinks" in any of the various scatter plots. (2) The sequence, however continuous, is by no means a homologous sequence. On the optical side, this nonhomology is obvious in the qualitative morphology, but can also be seen in the trend of some quantitative measures: from photometric data for a subset of the BST catalog, Bothun *et al.* (1986) give two different length scales for a galaxy, an exponential length scale D_L

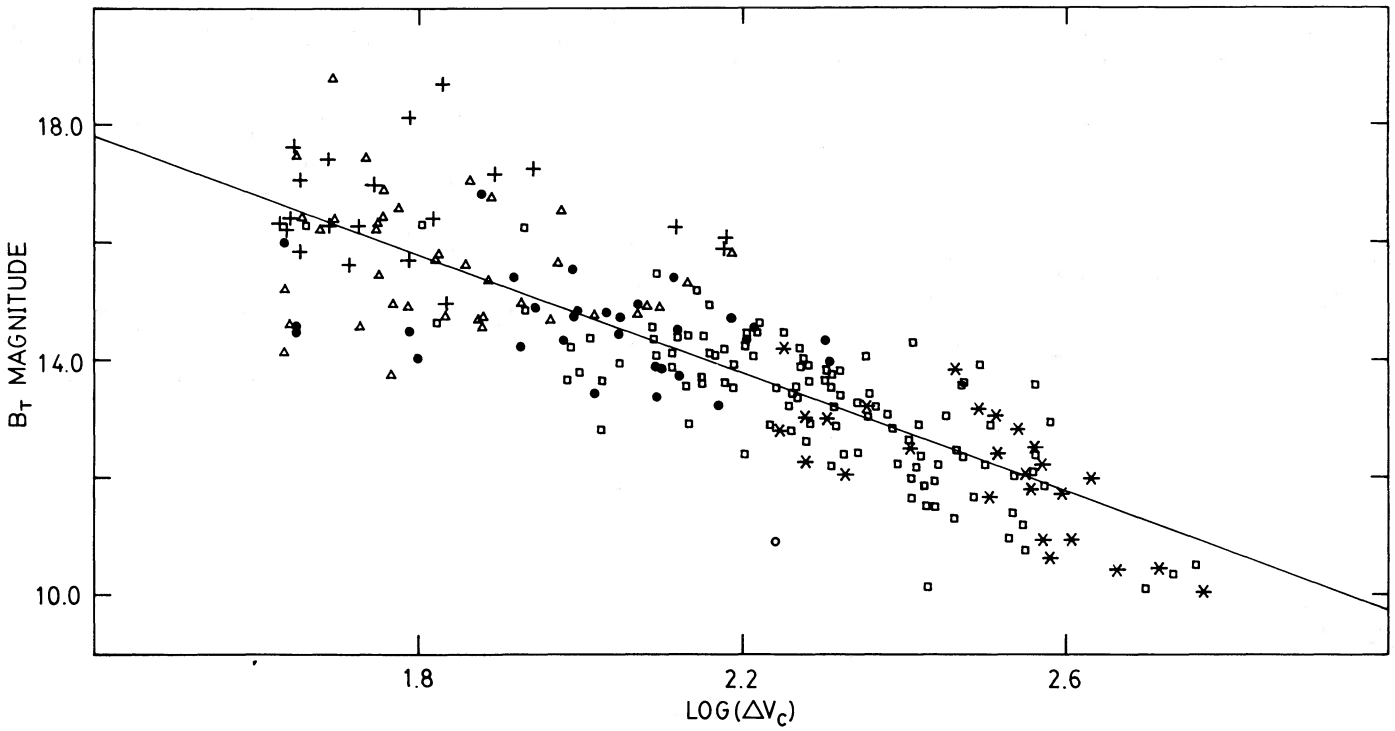

FIG. 7*a*

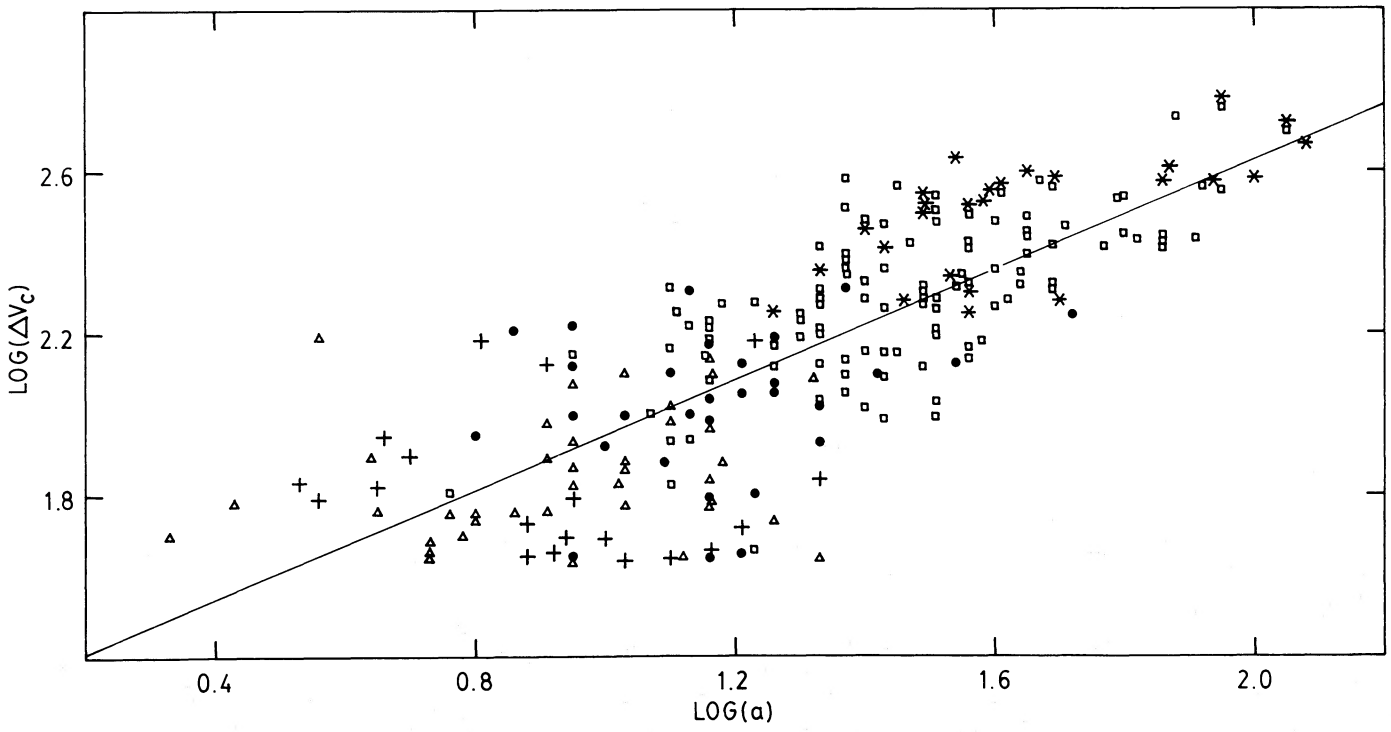

FIG. 7*b*

FIG. 7.—Tully-Fisher diagrams, (*a*) blue magnitude B_T vs. corrected H I profile width ΔV_c (*upper panel*), and (*b*) ΔV_c vs. optical diameter *a* (lower panel). Different morphological types are shown with different symbols; see Fig. 9 legend.

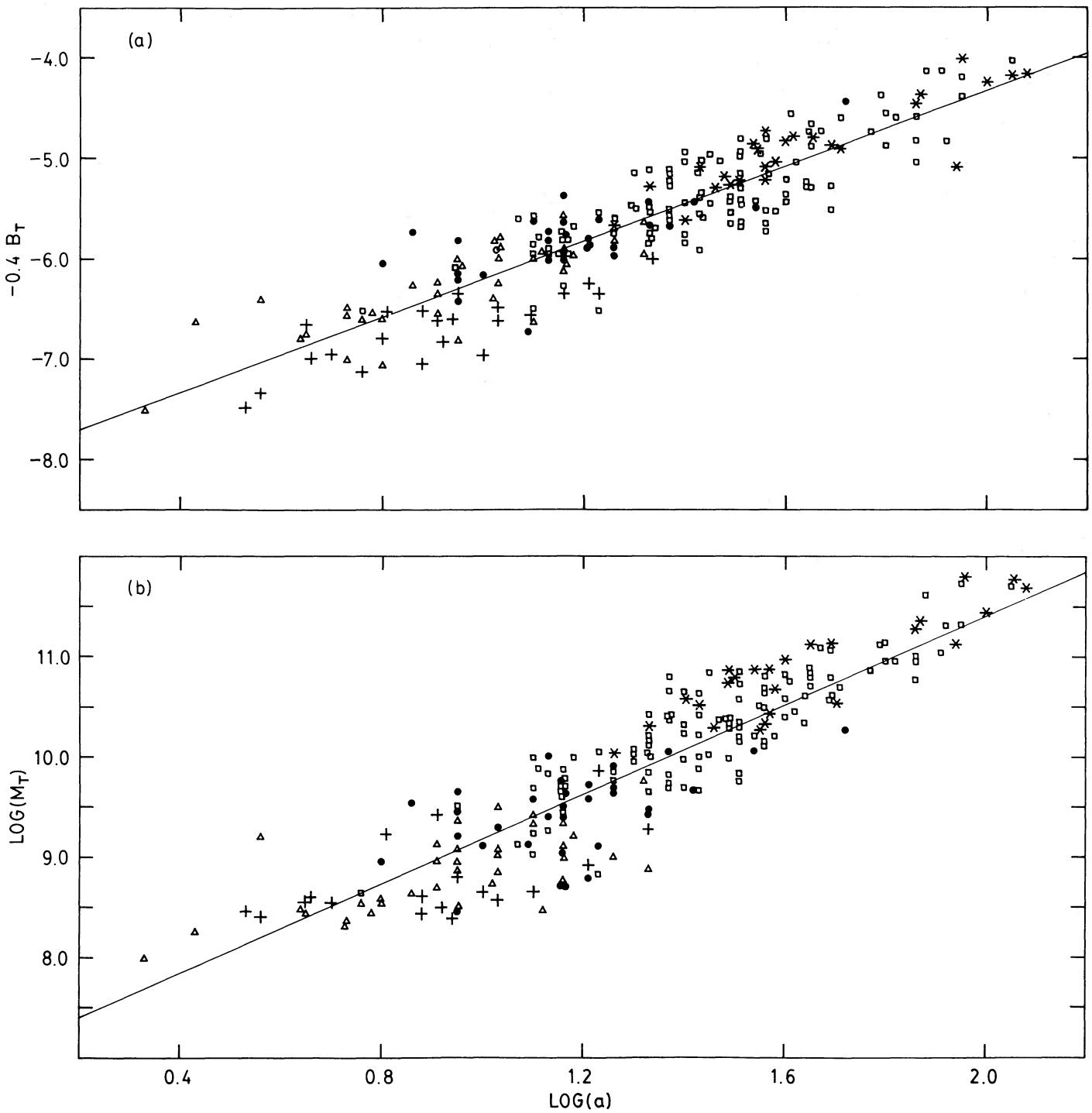

FIG. 8.—Scatter plots of (*a*) blue luminosity and (*b*) indicative gravitational mass vs. optical diameter *a*. Morphological types are shown with the same symbols used in Fig. 9.

(for the radial decrease of optical surface brightness), and an isophotal major diameter, which is similar to the outermost optical diameter a ($D_{\rm est}$ in BST). Along most of the sequence, the central surface brightness decreases strongly whereas the outer, mean surface brightness $\sigma_{\rm opt}$ remains almost constant; for the length scales, on the other hand, D_L is almost constant along the sequence (of order 20″), whereas the mean outer diameter a decreases (on average) with morphology. The H I spectra give two kinds of statistical information on dynamic trends, the overall velocity width ΔV and the fraction $f_{\rm DH}$ of double-horned profiles which is related to the ratio of rotational velocity $V_{\rm rot}$ to velocity dispersion $v_{\rm dis}$. Our data corroborate previous suggestions that $V_{\rm rot}$ decreases strongly along the sequence, whereas $v_{\rm dis}$ is almost constant from the largest giant spirals (Lewis 1987) to the faintest dwarfs. We have only preliminary H I mapping data from various authors (including

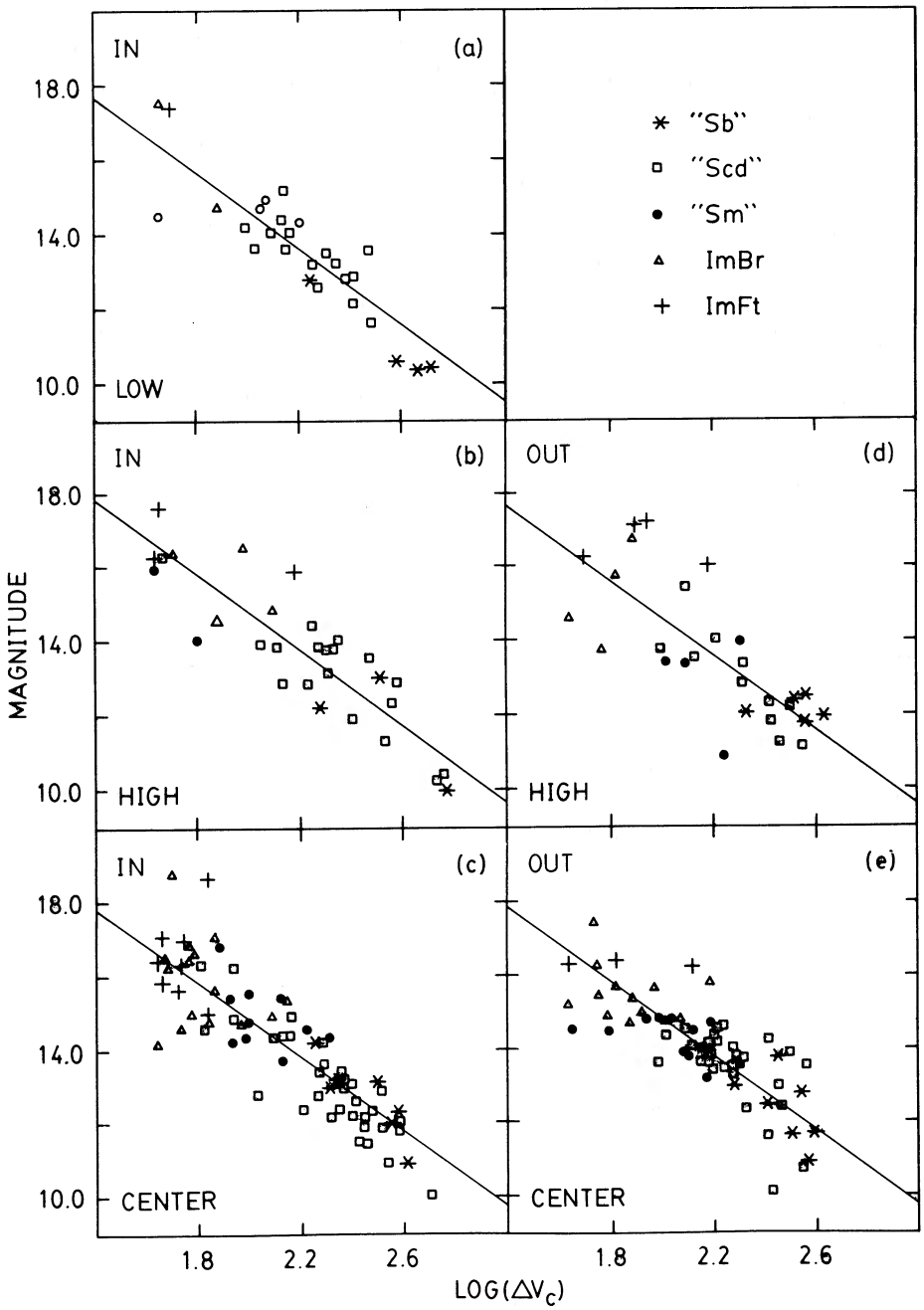

FIG. 9.—Tully-Fisher diagrams, blue magnitude vs. H I profile width, broken down by velocity range and location IN or OUT of the Virgo 5° core. The LOW, HIGH, and CENTER velocity ranges are the same as those used in Fig. 5 (L, H, and C, respectively). The slopes of the lines are constrained to be the same for all (see § VII), but the zero points are fitted separately. Magnitudes for OUT HIGH have been adjusted for distance (see § III).

ourselves), but find that H I diameters are usually larger than the optical a and are likely to correlate better with a than with D_L. Defining an indicative gravitational mass M_T in terms of the H I width ΔV and the optical diameter a, we find little variation in M_T/L along the sequence (on average); the ratio of hydrogen mass M_H to optical luminosity L increases only slowly along the sequence.

There is considerable scatter of various properties between individual galaxies, and considerable overlap between different morphological types. For instance, we have 15 Sc–Sd galaxies and 13 ImBr "dwarfs" in the same diameter range ($70'' < a < 100''$); the mean ΔV_c is (139 ± 11) km s^{-1} for the former and (95 ± 15) km s^{-1} for the latter, with a corresponding decline in f_{DH} from 0.67 to 0.38. In spite of the scatter, the correlation between size, mass, and specific angular momentum is quite clear. The exponent α and the correlation coefficient r are given in Table 6 for various quantities fit to a^{α}. Those fits involving the H I mass were obtained from OUT galaxies alone to minimize environmental effects. By way of comparison, Vigroux, Stasinska, and Comte (1987) find M_H

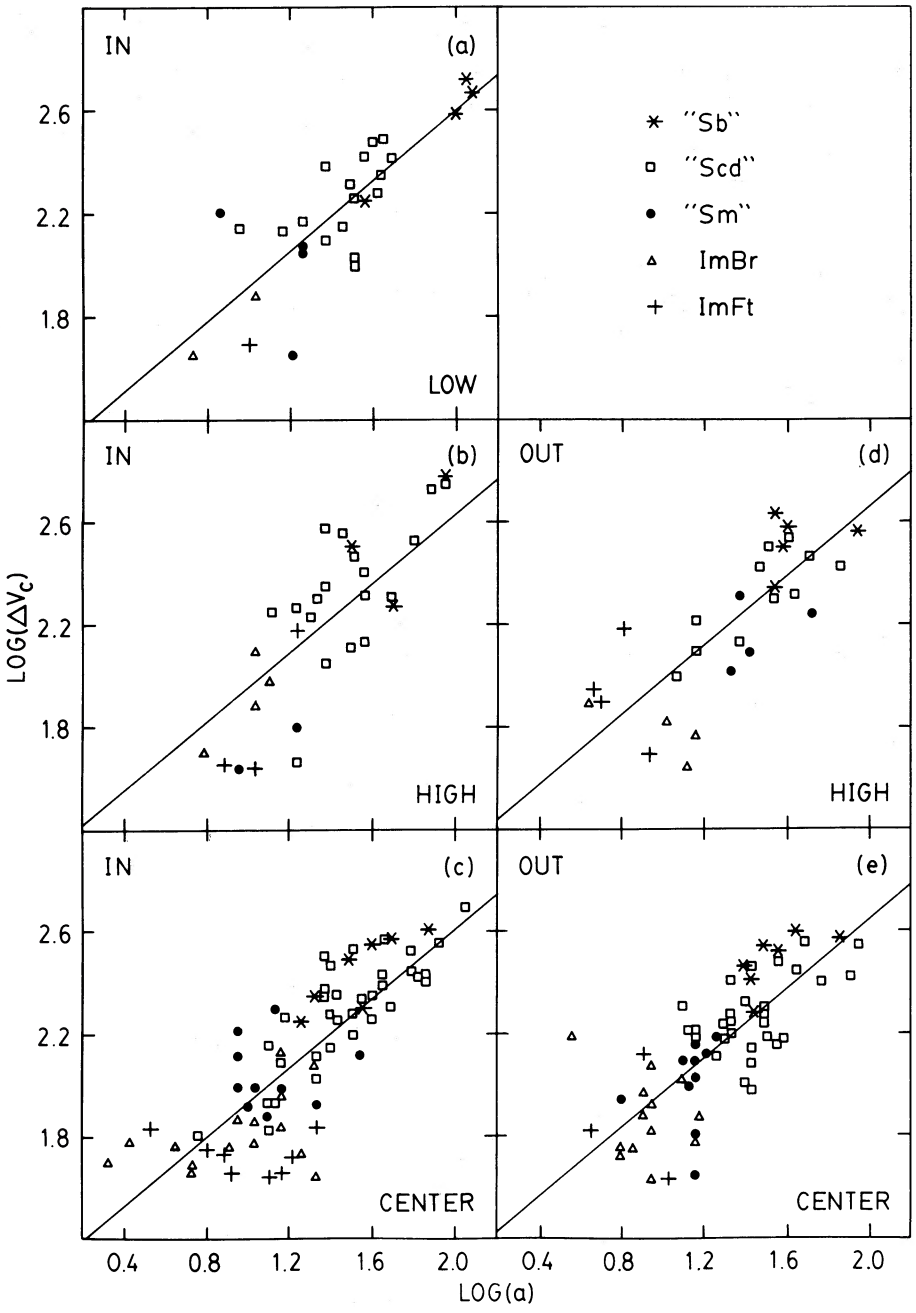

FIG. 10.—Same as Fig. 9, but for H I profile width vs. optical diameter. The diameters for OUT HIGH have been adjusted for distance (see § III).

TABLE 6

POWER LAW FITS TO a^{α}

Quantity	Power α	Correlation Coefficient
L	1.88	0.91
M_T	2.35	0.91
ΔV_c	0.68	0.79
M_T/L	0.49	0.45
σ_{opt}	−0.13	−0.15
σ_{MT}	0.35	0.32
σ_H	−0.19	−0.23
M_H/L	−0.23	−0.18
M_H/M_T	−0.72	−0.43

proportional to $L^{0.86}$ for an all-sky sample of mostly nearby dwarfs. The T-F relation along the whole sequence (from Sb to ImV) amounts to (for blue luminosity L)

$$L \propto \Delta V_c^{2.02} \quad (\text{with } r = 0.84)\,. \tag{5}$$

Note that the exponent 2.02 is appreciably smaller than the exponent 4 which would hold for a homologous sequence with all surface densities (mass and light) independent of the diameter a defining the sequence. This small exponent stems partly from the fact that the indicative mass surface density σ_{MT} in Table 6, defined as a constant times $\Delta V_c^2/a$, decreases with decreasing a, and partly from the increase of L/M_T.

Models for dwarf galaxy formation (e.g., Ikeuchi and Norman 1987) will have to account for the nonhomologous features in Table 6 and equation (5), as well as the increase of D_L/a along the series. On the observational side, more complete dynamical data is sorely needed for the faintest dwarf irregulars, where V_{rot} and v_{dis} become comparable and even the outer surface brightness σ_{opt} starts to decrease rapidly. The observational data in HHSGS for pure BCD galaxies and the theoretical stochastic star formation models (Gerola, Seiden, and Schulman 1980; Comins 1984) will be discussed in a forthcoming paper, as will the scatter in optical luminosity displayed in our present Figure 8.

Dekel and Silk (1986) have proposed a mechanism for biased galaxy formation wherein low-density peaks in the primordial matter distribution lose gas globally through supernova-driven winds, while the highest density peaks retain their gas. This model predicts that bright galaxies form preferentially in regions of greater galaxy number density (e.g. in clusters) while dwarfs form everywhere. The data discussed here are not ideally suited to test this hypothesis, since our OUT region is still in a moderately dense neighborhood. Better tests will follow when our survey of the void behind Virgo (Hoffman *et al.* 1988*b*; Lewis *et al.* 1988) is complete. However, to date we find no evidence (see Fig. 5 and discussion in § VI) that dwarf galaxies are more uniformly distributed than spirals (see also Thuan, Gott, and Schneider 1987). Regarding another environmental effect, we have seen that dwarf irregulars in the Virgo Cluster core are deficient in H I, but not greatly more than the spirals. Whether this absence of a stronger deficiency should be considered a theoretical puzzle or not will depend on more H I mapping of the dwarfs in the future: it is necessary to resolve the H I disks in order to find the true H I surface densities for dwarfs and to determine whether typical dwarf rotation curves rise or fall, which also affects the ratio of escape velocity to ΔV_c.

We acknowledge stimulating conversations and correspondence with B. Binggeli, G. Bothun, A. Dressler, J. Gallagher, R. Giovanelli, M. Haynes, B. M. Lewis, A. Sandage, S. Schneider, and T. X. Thuan. H. L. Williams assisted with some of the observations. B. Boetscher and K. Zadorozny drew the figures. This work was supported in part by US National Science Foundation grants AST 84-15162 at Cornell and AST 84-06392 at Lafayette, in part by the National Astronomy and Ionosphere Center which is operated by Cornell University for the National Science Foundation, and partially as part of the *IRAS* Extended Mission by the Jet Propulsion Laboratory, California Institute of Technology, under contract with the National Aeronautics and Space Administration.

REFERENCES

Aaronson, M., and Mould, J. 1983, *Ap. J.*, **265**, 1.
Binggeli, B. 1985, in *Star-forming Dwarf Galaxies and Related Objects*, ed. D. Kunth, T. X. Thuan, and J. Tran Thanh Van (Gif sur Yvette: Editions Frontieres), p. 53.
Binggeli, B., Sandage, A., and Tammann, G. A. 1985, *Astr. J.*, **90**, 1681 (BST).
Binggeli, B., Sandage, A., and Tarenghi, M. 1984, *A.J.*, **89**, 64.
Binggeli, B., Tammann, G. A., and Sandage, A. 1987, *A.J.*, **94**, 251 (BTS).
Bosma, A. 1985, *Astr. Ap.*, **149**, 482.
Bothun, G. D., Mould, J. R., Caldwell, N., and MacGillivray, H. T. 1986, *A.J.*, **92**, 1007.
Bothun, G. D., Mould, J. R., Wirth, A., and Caldwell, N. 1985, *A.J.*, **90**, 697.
Bottinelli, L., Gouguenheim, L., Paturel, G., and Teerikorpi, P. 1986, *Astr. Ap.*, **166**, 393.
Burstein, D., and Heiles, C. 1984, *Ap. J. Suppl.*, **54**, 33.
Chamaraux, P., Balkowski, C., and Gérard, E. 1980, *Astr. Ap.*, **83**, 38.
Comins, N. F. 1984, *Ap. J.*, **284**, 90.
Davies, R. D., and Lewis, B. M. 1973, *M.N.R.A.S.*, **165**, 231.
Dekel, A., and Silk, J. 1986, *Ap. J.*, **303**, 39.
de Vaucouleurs, G. 1961, *Ap. J. Suppl.*, **6**, 213.
de Vaucouleurs, G., and Corwin, H. G., Jr. 1986, *A.J.*, **92**, 722.
de Vaucouleurs, G., and de Vaucouleurs, A. 1973, *Astr. Ap.*, **28**, 109.
de Vaucouleurs, G., de Vaucouleurs, A., and Corwin, H. 1976, *Second Reference Catalogue of Bright Galaxies* (Austin: University of Texas Press) (RC2).
Dressler, A. 1986, *Ap. J.*, **301**, 35.
Farouki, R. T., Hoffman, G. L., and Salpeter, E. E. 1983, *Ap. J.*, **271**, 11.
Farouki, R. T., and Salpeter, E. E. 1982, *Ap. J.*, **253**, 512.
Feitzinger, J. V., and Galinski, T. 1986, *Astr. Ap.*, **167**, 215.
Fisher, J. R., and Tully, R. B. 1975, *Astr. Ap.*, **44**, 151.
———. 1981, *Ap. J. Suppl.*, **47**, 139.
Ftaclas, C., Fanelli, M. N., and Strubel, M. F. 1984, *Ap. J.*, **282**, 19.
Gaetz, T., Salpeter, E. E., and Shaviv, G. 1987, *Ap. J.*, **316**, 530.
Gallagher, J. S., III, and Hunter, D. A. 1984, *Ann. Rev. Astr. Ap.*, **22**, 37.
———. 1986, *A.J.*, **92**, 557.
Gerola, H., Seiden, P. E., and Schulman, L. S. 1980, *Ap. J.*, **242**, 517.
Giovanardi, C., Helou, G., Salpeter, E. E., and Krumm, N. 1983, *Ap. J.*, **267**, 35.
Giovanelli, R., and Haynes, M. P. 1985, *Ap. J.*, **292**, 404.
Giraud, E. 1986*a*, *Astr. Ap.*, **167**, 25.
———. 1986*b*, *Ap. J.*, **309**, 512.
Gisler, G. R. 1979, *Astr. Ap.*, **51**, 137.
Gordon, D., and Gottesman, S. T. 1981, *A.J.*, **86**, 161.
Grosbøl, P. J. 1985, *Astr. Ap. Suppl.*, **60**, 261.
Guiderdoni, B. 1987, *Astr. Ap.*, **172**, 27.
Guiderdoni, B., and Rocca-Volmerange, B. 1985, *Astr. Ap.*, **151**, 108.
Haynes, M. P., and Giovanelli, R. 1984, *A.J.*, **89**, 758.
———. 1986, *Ap. J.*, **306**, 466.
Haynes, M., Giovanelli, R., and Chincarini, G. 1984, *Ann. Rev. Astr. Ap.*, **22**, 445.
Helou, G., Giovanardi, C., Salpeter, E. E., and Krumm, N. 1981, *Ap. J. Suppl.*, **46**, 267.
Helou, G., Hoffman, G. L., and Salpeter, E. E. 1984, *Ap. J. Suppl.*, **55**, 433 (HHS).
———. 1987, in preparation.
Helou, G., Salpeter, E. E., and Krumm, N. 1979, *Ap. J. (Letters)*, **228**, L1.
Hewitt, J. N., Haynes, M., and Giovanelli, R. 1983, *Astr. J.*, **88**, 272.
Hoffman, G. L., Helou, G., Salpeter, E. E., Glosson, J. F., and Sandage, A. 1987, *Ap. J. Suppl.*, **63**, 247 (HHSGS).
Hoffman, G. L., Helou, G., Salpeter, E. E., and Lewis, B. M. 1988*a*, in preparation.
Hoffman, G. L., Lewis, B. M., Helou, G., Salpeter, E. E., and Williams, H. L. 1988*b*, *Ap. J. Suppl.*, submitted.
Hoffman, G. L., Salpeter, E. E., and Helou, G. 1985, in *IAU Symposium 117, Dark Matter in the Universe*, ed. J. Kormendy and G. R. Knapp (Dordrecht: Reidel), p. 162.
Huchra, J. 1984, private communication.
———. 1985, in *ESO Workshop on the Virgo Cluster*, ed. O.-G. Richter and B. Binggeli (Dordrecht: Reidel), p. 181.
Huchra, J. P., Davis, R. J., and Latham, D. W. 1984, in *Clusters and Groups of Galaxies*, ed. F. Mardirossian *et al.* (Dordrecht: Reidel), p. 79.
Huchtmeier, W. K., Seiradakis, J. H., and Materne, J. 1980, *Astr. Ap.*, **91**, 341.
———. 1981, *Astr. Ap.*, **102**, 134.
Ikeuchi, S., and Norman, C. A. 1987, *Ap. J.*, **312**, 485.
Kormendy, J. 1985, *Ap. J.*, **295**, 73.
Lea, S., and DeYoung, D. S. 1976, *Ap. J.*, **210**, 647.
Lewis, B. M. 1975, *Astr. Ap.*, **44**, 147.
———. 1984, *Ap. J.*, **285**, 453.
———. 1987, *Ap. J. Suppl.*, **63**, 515.
Lewis, B. M., Hoffman, G. L., Salpeter, E. E., and Helou, G. 1988, in preparation.
Lin, D. N. C., and Faber, S. M. 1983, *Ap. J. (Letters)*, **266**, L21.
Matteucci, F., and Chiosi, C. 1983, *Astr. Ap.*, **123**, 121.
Nilson, P. 1973, *Uppsala General Catalogue of Galaxies* (Uppsala: Acta Univeritatas) (UGC).
Richter, O.-G., and Huchtmeier, W. 1984, *Astr. Ap.*, **132**, 253.
Roberts, M. S. 1978, *A.J.*, **83**, 1026.
Sandage, A. 1983, in *IAU Symposium 100, Internal Kinematics and Dynamics of Galaxies*, ed. E. Athanassoula (Dordrecht: Reidel), p. 367.
———. 1986, *Astr. Ap.*, **161**, 89.
Sandage, A., and Binggeli, B. 1984, *A.J.*, **89**, 919.
Sandage, A., Binggeli, B., and Tammann, G. A. 1985, in *ESO Workshop on the Virgo Cluster*, ed. O. G. Richter and B. Binggeli (Garching: ESO), p. 239.
Sandage, A., and Tammann, G. A. 1976, *Ap. J.*, **210**, 7.
———. 1982, *Ap. J.*, **256**, 339.
Sarazin, C. L. 1986, *Rev. Mod. Phys.*, **58**, 1.
Skillman, E. D., and Bothun, G. L. 1986, *Astr. Ap.*, **165**, 45.
Stark, A. A., Knapp, G. R., Bally, J., Wilson, R. W., Penzias, A. A., and Rowe, H. 1986, *Ap. J.*, **310**, 660.
Tanaka, K. I. 1985*a*, *Pub. Astr. Soc. Japan*, **37**, 133.
———. 1985*b*, *Pub. Astr. Soc. Japan*, **37**, 427.

Thuan, T. X., Gott, J. R., and Schneider, S. E. 1987, *Ap. J. (Letters)*, **315**, L93.
Thuan, T. X., and Martin, G. E. 1981, *Ap. J.*, **247**, 823.
Thuan, T. X., and Seitzer, P. O. 1979, *Ap. J.*, **231**, 327.
Tully, R. B., and Fisher, J. R. 1977, *Astr. Ap.*, **54**, 661 (TF).
Tully, R. B., and Fouqué, P. 1985, *Ap. J. Suppl.*, **57**, 67.
Tully, R. B., and Shaya, E. J. 1984, *Ap. J.*, **281**, 31.
van Korkom, J., and Kotanyi, C. 1985, in *ESO Workshop on the Virgo Cluster*, ed. O.-G. Richter and B. Binggeli (Garching: ESO), p. 61.
Vigroux, L., Stasinska, G., and Comte, G. 1987, *Astr. Ap.*, **172**, 15.
Vigroux, L., Thuan, T. X., Vader, J. P., and Lachieze-Rey, M. 1986, *A.J.*, **91**, 70.
Warmels, R. H., and van Woerden, H. 1984, in *Clusters and Groups of Galaxies*, ed. F. Mardirossian, G. Giuricin, and M. Mezzetti (Dordrecht: Reidel), p. 251.

GEORGE HELOU: IPAC Mail Code 100-22, Caltech, Pasadena, CA 91109

G. LYLE HOFFMAN: Department of Physics, Lafayette College, Easton, PA 18042

E. E. SALPETER: Newman Laboratory, Cornell University, Ithaca, NY 14853